Environmental Health Perspectives
Vol. 73, pp. 77-90, 1987

Ovarian Neoplasia in the Sprague-Dawley Rat

by David J. Lewis*

Macroscopic and microscopic characteristics of 210 spontaneous ovarian tumors from 7748 Sprague-Dawley rats are described. The tumors were classified as tubular adenoma, anaplastic adenocarcinoma, papillary cystadenoma, papillary cystadenocarcinoma, mesothelioma, sertoliform tubular adenoma, Sertoli's cell tumor, granulosa cell tumor, thecal cell tumor, polycystic sex cord/stromal tumor, and lipoid cell tumor. The histogenesis of the tumor types is discussed.

Introduction

Spontaneous ovarian tumors are rare in most rat strains (*1–5*). The notable exception is the Osborne-Mendel strain, in which approximately 33% of rats over 18 months of age develop granulosa cell tumors (*6*). Reports describing more than just a few individual tumors are consequently rare. The sparsity of rat ovarian tumors and the lack of substantial reports are in contrast to the detailed and comprehensive knowledge of human tumors typified by several detailed reviews and classifications (*7–9*).

The classification of ovarian tumors is notoriously difficult in all species (*2*), and the low incidences of ovarian tumors in rats makes the diagnosis and classification especially difficult. These problems have prompted the opinion expressed by some workers that, except for a few well-described tumor types, it may be impossible to make precise diagnoses (*10*). These difficulties led to a recent detailed review of all ovarian tumors in the Huntingdon Research Centre (HRC) archives since 1978. This review (*11*) described 158 tumors from 5903 Sprague-Dawley rats, along with a suggested classification system. Since the publication of this review, ovarian tumors have continued to be monitored in our laboratory, and the present report describes the results of this continued work.

The classification system employed in this work is deliberately simple and based mainly on histological criteria with consideration of some histogenic factors. No attempt has been made to take clinical information into account, as data concerning endocrine function are not routinely available for rat ovarian tumors which are rarely suspected or diagnosed prior to death. The classification and diagnoses presented here are not, therefore, claimed to be the ultimate classification of rat ovarian neoplasia, but rather a reflection of the state of the art and a working model for future work and discussion.

*Department of Pathology, Huntingdon Research Centre, Huntingdon, Cambridgeshire, England.

Materials and Methods

All ovarian tumors from 7748 Sprague-Dawley rats (6338 CD, Charles River, Wilmington, MA, USA and 1410 CFY Anglia Laboratory Animals, Huntingdon, Cambridgeshire, UK) held in the HRC archives since 1975 were reviewed. The rats were untreated control animals from life-span carcinogenicity and toxicity studies. The majority of these studies ran for a minimum of 104 weeks. Both decedents and animals examined at termination were included.

At necropsy, a detailed macroscopic examination was performed, including macrophotography of unusual/representative lesions, and samples of a comprehensive range of organs and tissues, including ovaries fixed in 10% neutral buffered formalin. Samples were embedded in paraffin wax, sectioned at 5 μm, and routinely stained with hematoxylin and eosin (HE). Additional sections from selected tumors were stained by the periodic-acid-Schiff reaction (PAS), Alcian blue-PAS stain, Masson's trichrome, and reticulin stain. Frozen sections of selected tumors were stained with Oil-Red-O.

Results

The tumor types, incidences, and age relationship are given in Table 1. After consideration of clinical history, necropsy, and microscopic findings, pathologists in our laboratory assign factor(s) considered to be contributory to death for all animals that die or are killed *in extremis* during the course of a study. Examination of these factors revealed that ovarian tumors were considered contributory to death in only 16 cases out of a total of 210 ovarian tumors from 7748 rats. Most of these

Table 1. Age-related incidence of ovarian tumors in rats.

	Age ranges at death (weeks)								
	0–52	53–70	71–80	81–90	91–100	101–110	111–120	121–130	Total
A. Tumors of epithelial (ovarian coelomic mesothelium) origin									
Tubular adenoma	—	—	—	3	—	2	2	—	7
Anaplastic adenocarcinoma	—	—	1[a]	—	—	—	—	—	1
Papillary cystadenoma	—	—	—	—	—	2	—	—	2
Papillary cystadenocarcinoma	—	—	—	—	—	1[a]	—	—	1
Benign mesothelioma	—	—	—	1	—	1	—	—	2
Malignant mesothelioma	—	—	—	1	2	1	—	1	5[a]
B. Tumors of sex cord/stromal (mesenchymal origin)									
Sertoliform tubular adenoma	—	1	—	3	14	50	74	8	150
Sertoliform tubular adenocarcinoma	—	—	—	—	—	1	1	—	2
Sertoli's cell tumor	—	—	—	—	1	—	1	—	2
Granulosa cell tumor	—	—	—	—	2	7	4	2	15
Malignant granulosa cell tumor	1[a]	1	2[a]	—	1[a]	2	1[a]	—	8
Luteoma	—	—	—	—	—	1	—	—	1
Thecal cell tumor	—	—	—	1	—	—	3	5	9
Polycystic sex cord-stromal tumor	—	1[a]	—	2[a]	—	—	1[a]	—	4
Lipoid cell tumor	—	—	—	—	—	—	1	—	1
								Total	210

[a]Tumors considered as factors contributory to death of the animal.

cases involved malignant tumors (Table 1). Of the remaining ovarian tumors, few caused detectable clinical signs, and most were unsuspected prior to necropsy. No significant differences were detected between rats from the two sources.

Tubular Adenoma

Macroscopically, tubular adenomas were usually detected as firm, pale masses and ranged in size from 5 to 20 mm (Table 2). Microscopically, the tumors were composed of simple invaginations of the surface epithelium in the form of narrow tubules lined by cuboidal cells (Plates 1 and 2). Nuclei were generally round, with few mitoses. Focal evidence of tubular branching was detected. Along the tumor surface, and occasionally in cysts, many of the epithelial cells, from all tumors, contained prominent, round, homogeneous, eosinophilic, PAS positive, cytoplasmic inclusions that also stained positively with phloxine-tartrazine. Focally, in some tumors, short, irregular papillary projections from the tumor surface were present. These were continuous with both the surface epithelium and the underlying tubular structures. Occasionally, traces of Alcian blue positive material were detected in the lumina. The interstitium contained variable numbers of densely packed cells which resembled granulosa cells, but lacked the characteristic nuclear chromatin pattern. This sometimes resulted in a complex admixture of epithelial tubules and interstitial cells, in which the former were sometimes difficult to identify. Thinner sections, cut at

Table 2. Tubular adenomas: necropsy findings.

Case number	Tumor location	Description
1	Right ovary	Firm, white mass, 7 mm diameter
2	Right ovary	Firm mass, 8 × 6 × 5 mm
3	Right ovary	Firm, white nodule, 5 mm diameter
4	Left ovary	Mass, 12 mm diameter
5	Left ovary	Pale mass, 6 × 6 × 5 mm
6	Right ovary	Pale, nodular mass, 20 mm diameter
6	Left ovary	Enalrged, 5 mm diameter
7	Left ovary	Serosanguineous fluid-filled cyst, 48 × 34 × 24 mm, containing a mass, 22 × 20 × 14 mm

3 μm, were useful in these cases, as were reticulin-stained preparations.

Anaplastic Adenocarcinoma

At necropsy, this single neoplasm was detected as a cream mass (16 × 12 × 9 mm) in the right ovary. The tumor was composed of poorly differentiated tubules and acini (Plates 3 and 4), and the cells demonstrated nuclear pleomorphism and prominent mitoses. The tubular basement membrane was often indistinct. The tubular cells were irregularly arranged, with prominent multilayering. There were abundant reactive stroma and prominent infiltration of neutrophils, with areas of necrosis. The tumor had infiltrated periovarian tissue, but distant metastases were not detected.

Papillary Cystadenoma

Macroscopically, one of these two tumors was detected as a cyst 7 mm in diameter, the other as a 5 mm diameter nodule. Both neoplasms consisted of a simple cyst filled with complex papillomatous projections. Little nuclear pleomorphism and few mitoses were detected. The cells had round nuclei and sparse cytoplasm. The cysts contained amorphous eosinophilic material, which stained negatively with mucin stains.

Papillary Cystadenocarcinoma

At necropsy, this tumor appeared as a cystic mass of the left ovary (30 × 22× 19 mm), with a few nodules (up to 5 mm diameter) on the peritoneal surfaces and a few milliliters of serosanguineous fluid in the abdomen. Microscopically, the tumor had definite adenomatous and papillomatous patterns with cystic spaces. The cuboidal cells were arranged in acini and papillomatous projections with areas of multilayering. Occasionally, mitoses and slight nuclear pleomorphism were detected. The peritoneal metastases were microscopically identical to the primary tumor.

Mesothelioma

The two mesotheliomas classified as benign were not detected at necropsy. These tumors were composed of superficial papillary projections from the ovarian surface. The cells were cuboidal, with round nuclei and few mitoses and continuous with cells of the ovarian surface epithelium. The lesions were multifocal.

Malignant mesotheliomas were present macroscopically as large masses (≤ 70 × 55 × 42 mm), with variable numbers of nodules throughout the peritoneal cavity and serosanguineous fluid in the abdomen (Table 3). The tumors were all characterized microscopically by a pronounced tubulopapillary pattern (Plate 5), sometimes with stromal hyalinization. The implantation metastases (Plate 6) were similar to the primary tumors but frequently were only superficial deposits, rarely demonstrating invasive growth into the underlying tissue. Metastatic deposits were found in the lungs of one case.

Table 3. Malignant mesotheliomas: necropsy findings.

Case number	Tumor location	Description
1	Left ovary	Firm, pale mass, 22 × 12 × 9 mm
	Liver	Left lobe, dark subcapsular area, 10 mm diameter
2	Right ovary	Pale, firm mass, 30 × 24 × 20 mm
	Left ovary	Pale, firm mass, 24 × 13 × 12 mm
	Peritoneum	Multiple pale, firm nodules, up to 10 mm diameter
	Abdomen	Approximately 15 mL serosanguineous fluid
3	Left ovary	Pale nodular mass, 57 × 27 × 25 mm
	Right ovary	Mass, 13 × 13 × 6 mm
	Peritoneum	Multiple pale nodules, up to 5 mm diameter
	Abdomen	A few milliliters serosanguineous fluid
4	Right ovary	Pale, firm mass, 41 × 39 × 36 mm
	Peritoneum	Multiple pale, firm excrescences, up to 5 mm diameter
	Abdomen	Serosanguineous fluid
5	Right ovary	Cystic, bosselated mass, 70 × 55 × 42 mm
	Peritoneum	A few firm excrescences, up to 7 mm diameter

Sertoliform Tubular Adenoma

At necropsy, these tumors were characterized as discernible pale/white nodules or masses (Plate 7), generally within the size range of 2 to 10 mm (Table 4). The tumors were composed of variable numbers of pale tubules (Plates 8 and 9) and either formed simple round/oval profiles or complex digitating profiles. The tubules were usually solid, although occasionally, accumulations of eosinophilic, PAS-positive material were present in the center. The tubules were composed of pale, weakly eosinophilic cells with indistinct cell boundaries, giving a syncytial appearance. Variable numbers of round eosinophilic, PAS-positive inclusions which resembled hyaline droplets, and vacuoles (lipid) were present in the cytoplasm. Nuclei were round or oval and occasionally had densely stained grooves. A few mitoses were detected in some tumors. The tubules had a distinct basement membrane with a fine peritubular stroma. The density of the discernible tubular elements varied within individual tumors, with a corresponding amount of stromal cells. Reticulin staining emphasized the tubular pattern and also revealed groups of stromal cells surrounded by reticular fibers. The tumor nodules were usually well-circumscribed and demarcated from the remaining ovarian tissue, which sometimes appeared compressed. Occasionally, tumors were detected in which the entire ovary was replaced by neoplastic tubules.

Table 4. Sertoliform tubular adenomas: necropsy findings from typical cases.

Case number	Tumor location	Description
1	Left ovary	Firm, white mass, 5 mm diameter
2	Right ovary	Pale mass, 8 × 6 × 5 mm
	Left ovary	Pale mass, 9 × 8 × 7 mm
3	Right ovary	Pale mass, 10 × 10 × 6 mm
4	Right ovary	Yellow nodule, 3 mm diameter
5	Right ovary	Firm, pale nodule, 4 mm diameter
	Left ovary	Firm, pale nodule, 5 mm diameter
6	Right ovary	Pale mass, 5 mm diameter
7	Right ovary	Enlarged, white
8	Right ovary	Firm, pale mass, 7 × 5 × 4 mm
	Left ovary	Firm, pale mass, 5 × 5 × 3 mm
9	Right ovary	Pale, firm mass, 3 mm diameter
	Left ovary	Pale, firm mass, 2 mm diameter
10	Left ovary	Pale mass, 19 × 13 × 12 mm
11	Right ovary	Firm, white nodule, 4 mm diameter
12	Right ovary	Firm yellow
	Left ovary	Firm yellow
13	Right ovary	Pale mass, 3 × 3 × 2 mm
14	Left ovary	Pale, firm mass, 6 × 5 × 4 mm
15	Left ovary	Mass, 8 mm diameter
	Right ovary	Mass, 10 mm diameter

In two cases, infiltration of tubular elements into periovarian tissues was detected, and these lesions were classified as malignant. Little nuclear pleomorphism and no detectable increase in mitotic activity were observed. These tumors were both from the left ovary and were measured as 15 mm diameter and 15 × 9 × 7 mm at necropsy.

Sertoli's Cell Tumor

Both tumors originated as masses in the right ovary and were 20 and 30 mm in diameter. Microscopically the tumors varied. One tumor had a well-defined pattern of tubules lined by a single layer of columnar/cuboidal cells with pale cytoplasm (Plates 10 and 11). The other tumor was composed of an admixture of three distinct components (Plates 12 and 13). The tumor had prominent palisaded columnar cells and fine fibrovascular septae. At the center of the palisaded cells were polygonal cells with pale or clear cytoplasm and occasionally, accumulations of eosinophilic, PAS-positive material. Solid tubules, usually elongated, occasionally round or oval in profile, with basally located nuclei, were present. The apical cell margins were indistinct and appeared to be composed of fine intertwining fibrils. Tubules that resembled those of the sertoliform tubular adenomas were present (Plate 13).

Granulosa Cell Tumor

Macroscopically, these neoplasms were variable in size (from 1 mm diameter to 54 × 44 × 40 mm) and were contained within the distended bursa (Plate 14), (Tables 5 and 6). Evidence of hemorrhage was occasionally a feature. Histologically, the tumors were similar to those of other species. Several patterns were present. In the follicular form, intrafollicular spaces contained eosinophilic, PAS-positive material. The solid form was characterized by solid sheets of uniform cells, broken only occasionally by blood vessels. The trabecular pattern was distinguished by palisaded cells surrounded by connective tissue septae. The oval cells of the diffuse (sarcomatous) type were slightly elongated and resembled thecal cells, but reticulin staining demonstrated reticular fibers around groups of cells rather than around individual cells. Call-Exner bodies were not a prominent feature in rats. Many, particularly larger, granulosa cell tumors contained areas of hemorrhage and necrosis with siderocytes and lipofuscin granules.

Malignant granulosa cell tumors showed local invasion and/or distant metastases to the kidneys, lungs, and lymph nodes. One tumor contained areas of large lutein cells (Plates 15 and 16) in the primary but only typical granulosa cells were present in the pulmonary metastases (Plate 17).

Luteoma

A single luteoma arising as a mass in the left ovary measured 10 mm in diameter at necropsy. The tumor cells resembled highly luteinized granulosa cells.

Table 5. Granulosa cell tumors: necropsy findings.

Case number	Tumor location	Description
1	Right ovary	Red nodule, 1 mm diameter
2	Left ovary	Dark, edematous mass, 40 × 40 × 16 mm
3	Right ovary	Pale mass, 5 × 5 × 4 mm
4	Right ovary	Firm, hemorrhagic mass, 54 × 44 × 40 mm
5	Left ovary	Firm mass, 24 × 24 × 22 mm
6	Left ovary	Pale mass, 7 × 6 × 5 mm
7	Left ovary	Dark mass, 12 mm diameter
8	Left ovary	Firm, pale, hemorrhagic mass, 28 × 22 × 19 mm
9	Right ovary	Hemorrhagic mass, 10 × 9 × 7 mm
10	Left ovary	Dark mass, 7 mm diameter
11	Right ovary	Firm, hemorrhagic mass, 15 × 12 × 9 mm
12	Right ovary	Hemorrhagic mass, 12 mm diameter

Table 6. Malignant granulosa cell tumors: necropsy findings.

Case number	Tumor location	Description
1	Left ovary	Grossly enlarged, cystic, 30 × 23 × 20 mm
	Lumbar lymph nodes	Enlarged and hemorrhagic, 30 × 30 × 22 mm
	Lungs	Left lobe, subpleural mass, 14 × 14 × 11 mm
2	Right ovary	Firm, hemorrhagic mass, 54 × 45 × 40 mm
3	Right ovary	Hemorrhagic, cystic mass, 21 × 15 × 7 mm
	Right kidney	Dark, subcapsular mass, 7 mm diameter
4	Left ovary	Hemorrhagic mass, 21 mm diameter
5	Right ovary	Mass, 13 × 11 × 10 mm
	Lungs	Several dark, subpleural nodules, up to 5 mm diameter
6	Right ovary	Hemorrhagic mass, 34 × 21 × 19 mm
	Lungs	left lobe, subpleural mass, 10 mm diameter
7	Left ovary	Cystic mass, 23 × 17 × 9 mm
	Left kidney	Cystic, subcapsular mass, 15 mm diameter
8	Left ovary	Mass, 10 mm diameter

Table 7. Thecal cell tumors: necropsy findings.

Case number	Tumor location	Description
1	Right ovary	Pale, firm mass, 10 mm diameter
2	Left ovary	Mass, 44 × 35 × 30 mm
3	Right ovary	Firm mass, 31 × 26 × 17 mm
4	Right ovary	Pale mass, 10 × 10 × 6 mm
5	Left ovary	Mass, 10 mm diameter
6	Right ovary	Pale, firm mass, 9 mm diameter
7	Left ovary	Firm mass, 15 × 14 × 10 mm

Thecal Cell Tumor

These tumors showed considerable variation in size (Table 7). Some thecal cell tumors were detected only at microscopy, whereas others formed large masses (up to 44 × 35 × 30 mm). Microscopically, thecomas were composed of densely packed fusiform cells, usually arranged in pronounced whorled patterns, giving a nodular appearance (Plates 18–20). The fusiform cells exhibited distinct pericellular reticular fibers and contained variable lipid. Mature collagen fibers were sparse in small tumors. In larger neoplasms, extensive necrosis was often present, with only perivascular persistence of viable tissue. Focal areas of mineralization were also a common feature of the larger tumors. Areas of hyalinization were occasionally present in some tumors, but in one small tumor were extensive, with areas of apparent osteoid and chondroidlike differentiation.

Polycystic Sex Cord-Stromal Tumor

Macroscopically, four tumors were identified as large polycystic masses (Table 8, Plate 21). These tumors were virtually identical in structure, with large cystic spaces lined by flattened cells and narrow interstitial stroma composed of loosely packed cells showing focal luteinization (Plates 22 and 23). The cells could not be identified as thecal nor granulosa cells. Reticulin staining demonstrated reticular fibers around both groups of cells and individual cells. In two tumors, peritoneal metastases identical in structure to the primary were present.

Lipoid Cell Tumor

A single lipoid cell tumor was detected macroscopically as a nodule (13 mm diameter) adjacent to the hilus. Microscopically, the tumor was composed of large, round eosinophilic cells, often with large vacuoles.

Secondary Tumors

The ovaries were involved in cases of lymphoma, but true metastatic deposits were extremely rare. Ovarian involvement was detected in five cases of generalized abdominal mesothelioma in which ovarian deposits were identical to those elsewhere in the abdomen.

In this series, the ovaries were the site of only one metastatic tumor: a pancreatic adenocarcinoma that had spread throughout the abdominal cavity. Coincidentally, the ovary involved was the site of a granulosa cell tumor.

Discussion

Some workers have considered true tubular adenomas unique to the mouse ovary (*12*). In mice, tubular adenomas have been shown to originate from downgrowths of the surface epithelium (*4,13–15*).

Murine tubular adenomas with prominent granulosalike interstitial cells have been termed "complex tu-

Table 8. Polycystic sex cord-stromal tumors: necropsy findings.

Case number	Tumor location	Description
1	Right ovary	Polycystic mass, 90 × 65 × 50 mm
2	Left ovary	Cystic, hemorrhagic mass, 29 × 25 × 20 mm
	Abdominal adipose tissue	Multiple cystic, nodular masses, up to 7 × 6 × 5 mm
3	Right ovary	Polycystic mass, 55 × 55 × 45 mm
	Omentum	Soft, pale nodules, up to 1 mm diameter
	Diaphragm	Soft, pale nodules up to 1 mm diameter
4	Right ovary	Polycystic mass, 20 × 31 × 15 mm

bular adenomas" (*13–15*). Granulosa cell tumors are reported to possibly develop from complex tubular adenomas (*14,16*). Complicated adenomatous and tubular patterns have been described in granulosa cell tumors (*2,3,*). These tumors presented considerable diagnostic problems and the researchers suggested that when such components formed a large part of a tumor, alternative diagnoses should be considered.

The recent identification of two clear examples of tubular adenomas in rats and the association with granulosa cell tumors in mice led to a detailed review of all granulosa cell tumors. During this review, five tumors were identified in which tubular elements were admixed with prominent granulosalike cells. Alcian blue staining, shown to be useful in the differentiation of murine complex tubular adenomas and granulosa cell tumors (*15*), confirmed the tubular presence. The continuity of some tubular elements with the surface epithelium suggests that surface epithelium is a likely origin. A constant feature of these tumors was cytoplasmic inclusions. Similar inclusions were not detected in granulosa cell tumors, nor in malignant mesotheliomas. The origin of these inclusions is uncertain. There are two obvious suggestions: inclusions represent a storage of products of intracellular synthesis and the accumulation of an absorbed extracellular material. Ovarian mesothelial cells are known to be capable of phagocytosis (*17*). Whatever their origin, these inclusions would at present appear of diagnostic value for tubular adenomas in rats.

The single tumor classified as an anaplastic adenocarcinoma was histologically similar to those induced in rats by the clipping method with 7,12-dimethylbenz-(a)anthracene (*18,19*). The tumor strongly resembled neoplasms of the uterine endometrium occasionally encountered in our rats and may represent the equivalent of the endometrioid adenocarcinoma reported in women (*7–9,20*).

Papillary cystadenomas are rare in rats at HRC (*11*), only two cases were detected. The single malignant counterpart metastasized by transcoelomic spread. Similar tumors have been reported previously (*21,22*), but are rare. In women, such tumors account for approximately 90% of all ovarian cancers (*8*); they are relatively common in old hens (*4,12,23,24*), and they are also relatively common in dogs (*23,25*).

The nomenclature of the epithelial ovarian tumors is controversial (*26*), particularly the terminology of serous adenocarcinomas and mesotheliomas. It is generally accepted that most if not all of the epithelial ovarian tumors arise from the surface epithelium (*8,25*). There is also general agreement that this epithelium is in fact a modified mesothelium (*25,26*). It has been suggested that many of the human epithelial ovarian tumors are in fact mesotheliomas (*26*) that demonstrate various forms of differentiation of the pluripotent Müllerian epithelium (*27,28*). However, in view of the long-established and entrenched epithelial/adenoma/adenocarcinoma terminology, these terms have been used in the present work.

The diagnosis of mesothelioma was reserved for cases which were histologically indistinguishable from other mesotheliomas, such as those arising from the tunica vaginalis, the abdominal coelomic mesothelium (generalized abdominal mesothelioma), and the pleura. Although in human classification mesotheliomas are rarely included, a few isolated cases have been described (*29*).

Tubular structures which resemble seminiferous tubules with Sertoli-like cells but are devoid of spermatogenic tissue are commonly encountered in the ovaries of aged rats and mice (*10,30–34*). Tubular adenomas composed of these Sertoli-like cells have been described in rats by several workers both as spontaneous (*23,32*) and induced (*35,36*) neoplasms. In order to distinguish between tubular adenomas of this sertoliform differentiation and the tubular adenomas composed of cuboidal downgrowths of the surface epithelium, the term "sertoliform tubular adenoma" has been adopted. The sertoliform tubules have been induced by hypophysectomy and were considered to be related to gonadotropin deficiency (*30,32,37*). A decrease in the relative number of gonadotropin-producing cells has been demonstrated in the pituitary of aging anestrous rats (*38*).

Similarly decreased levels of LH and FSH have been measured in aging rats (*39,40*). These tubules may therefore be regarded as an indication of secondary ovarian senescence (*30*). Furthermore, if their apparent Sertoli differentiation is correct, these tubules may represent a manifestation of latent androgenic ovarian potential following loss of gynecoid influences (*32*). Similar tumors have been classified as Sertoli's cell neoplasms by some authors (*10*). Following administration of human chorionic gonadotropin, the tubules undergo luteinization, with an ultrastructural appearance suggestive of steroidogenesis (*37*). However, no histological evidence of hormonal activity has been found in any tissues.

The differential diagnosis of hyperplasia and adenomas of these sertoliform tubules is difficult because of the diffuse nature of the lesion. However, when the tubular proliferation becomes extensive, with macroscopically detectable enlargement and nodule or mass formation, other ovarian structures become replaced or compressed; the tubules form a microscopically distinct nodule or mass, and a neoplastic diagnosis is considered not inappropriate. The histogenesis of sertoliform tubules is uncertain (*36*); possible origins include granulosa cells (*34,37*), tubular surface epithelial downgrowths (*13,15*), rete-ovarii (*13*), residual hilar medullary tissue (*36*), persisting embryonic influences (*35*), or deficiency cells (*37*). It is possible to find apparent evidence suggestive of origins from rete ovarii, tubular epithelial downgrowths, follicles, and deficiency cells, thus, the histogenesis remains obscure. The vivid multipotency typical of the embryonic period demonstrated in mature ovarian tissues of mice (*13*) may offer at least a partial explanation for the problem.

Some reports have failed to find evidence of mitoses in sertoliform tubules (*37*), and few others have commented on their presence. However, the present study

has clearly shown mitoses in the tubular cells. Thus, once formed, the tubules are capable of self-replication.

In the previous report (*11*), sertoliform tubular adenomas were classified as of epithelial origin. However, their strong resemblance to rudimentary seminiferous tubules with Sertoli's cells and their reported ability to undergo luteinization have prompted their tentative reclassification as sex cord-stromal tumors.

Sertoli's cell tumors are rare in all species. The two tumors classified as Sertoli's cell neoplasms differed in pattern. One was composed of distinct tubules. Sertoli's cell tumors in dogs and women exhibit a range of histological appearances (*8,41,42*). Differentiation from granulosa cell tumors is not always conclusive (*22,25,42*), and an unclassified category of sex cord-stromal tumor may be necessary (*9*).

Little morphological evidence of hormonal activity was detected in any tumors of this series. Nonluteinized granulosa cells may be functionally inert (*43*), whereas luteinized cells may produce progesterone (*44*). The possibility of a correlation between absence of hormonal activity and the generally low incidence of luteinization was considered. However, even in cases in which luteinization did occur, no features of hormonal activity were detected. In some cases of induced granulosa cell tumors, endocrine hyperactivity has been shown to be possibly related to reactive nonneoplastic theca-lutein cells (*45*).

Endometrial hyperplasia has been reported in rats (*3*) and mice (*33*) with granulosa cells tumors, but hyperplasia is a relatively common finding in aged rats in our laboratory, and therefore, factors other than ovarian tumors appear more influential in its development. Granulosa cell tumors with several different patterns were all composed of well-differentiated cells that resembled normal granulosa cells, and even the malignant forms were well differentiated. These tumors were characterized by local invasive growth and/or distant metastases.

In rats, tumors of the granulosa-thecal cell types appear less mixed than in some other species, and no cases were considered to warrant the diagnosis of mixed granulosa-thecal cell tumor. Thecal cell tumors were the third most common tumor type and similar histologically to those of other species. The differential diagnosis of thecoma and fibroma is often difficult (*7,8*), but the presence of hyalinization, whorled pattern, tendency to nodular growth, pericellular reticulin fibers, and lipid-rich cytoplasm favors a diagnosis of thecoma (*2,3*). These criteria were used in the present study, and no cases of fibroma were seen. The single thecoma with pronounced areas of hyalinized ground substance with areas of osteoid and chondroidlike differentiation would appear to be analogous to some forms reported in women (*41*).

The four tumors designated cystic sex cord-stromal tumors were all characterized by a grossly polycystic appearance with a slightly loose stroma, focally abundant lipid, and both pericellular and nonpericellular reticulin patterns. Although only a low mitotic rate and little nuclear pleomorphism were demonstrated, the malignant nature was confirmed by peritoneal metastases in two cases. In the literature, the only similar tumor traced in rats was characterized by clefts rather than cysts and was tentatively classified as a thecal cell tumor (*3*). The presence of four cases in this series suggests a definite entity and warrants separate classification, under a descriptive term, until the histogenesis can be elucidated.

Reports of lipoid cell tumors in rats have not been traced. This tumor type is believed to arise from Leydig cells, lutein cells, or adrenal rests (*7–9*). The histogenesis of the single lipoid cell tumor detected in this series could not be determined conclusively. However, the tumor's apparent extraovarian location adjacent to the hilus suggests an adrenal rest origin (*8*). Unlike humans, adrenal rests are rarely observed in rats, but may occasionally be seen in cats (*25*).

No cases of ovarian carcinoid were detected in this series. Argentaffin and arygyrophilic reactions were performed on several of the tumors, but proved negative (as did the search for dense-core neurosecretory granules by retrospective electron microscopy).

Although dysgerminomas have been reported in the mouse (*33*) and in dogs and cats (*46*), no cases have been traced in rats. Similarly, teratomas were not encountered in the present study, and only a single case has been traced in the literature (*47*).

The author thanks W. A. Gibson, R. L. Gregson, and C. Gopinath for assistance and helpful comments; M. W. Cannon for photographic help; and A. Galloway for secretarial assistance.

REFERENCES

1. Altman, N.H., and Goodman, D. G. Neoplastic diseases. In: The Laboratory Rat, Vol. 1 (H. J. Baker, J. R. Lindsey, and S. M. Weisbroth, Eds.), Academic Press, London, 1979, pp. 333–376.
2. Carter, R. L. Pathology of ovarian neoplasms in rats and mice. Eur. J. Cancer 3: 537–543 (1968).
3. Carter, R. L., and Ird, E. A. Tumours of the ovary. In: Pathology of Tumours in Laboratory Animals, Vol. 1, The Rat (V. S. Turusov, Ed.), IARC, Geneva, 1978, pp. 189–194.
4. Lingeman, C. H. Etiology of cancer of the human ovary: a review. JNCI 53: 1603–1618 (1974).
5. Russfield, A. B. Tumors of endocrine glands and secondary sex organs. Public Health Service Publication No. 1332, 1966, pp. 45–56.
6. Snell, K. Spontaneous lesions of the rat. In: The Pathology of Laboratory Animals (W. E. Ribelin and J. R. McCoy, Eds.), C.C. Thomas, Springfield, IL, 1965, pp. 241–300.
7. Langley, F. A. The Pathology of the Ovary. In: Postgraduate Obstetrical and Gynaecological Pathology (H. Fox and F. A. Langley, Eds.), Pergamon, Oxford, 1973, pp. 187–243.
8. Scully, R. E. Ovarian tumours. A review. Am. J. Pathol. 87: 686–720 (1977).
9. Serov, S. F., Scully, R. E., and Sobin, L. M. International Histological Classification of Tumors, No. 9. Histological Typing of Ovarian Tumors. WHO, Geneva, 1973.
10. Greaves, P., and Faccini, J. M. Rat Histopathology. Elsevier, Amsterdam, 1984, pp. 171–186.
11. Gregson, R. L., Lewis, D. J., and Abbott, D. P. Spontaneous ovarian neoplasms of the laboratory rat. Vet. Pathol. 21: 292–299 (1984).
12. Squire, R. A., Goodman, D. G., Valerio, M. G., Fredricksen, T., Strandberg, J. D., Levitt, M. M., Lingeman, C. H., Harshbarger,

J. C., and Dawe, C. J. Tumors. In: Pathology of Laboratory Animals, Vol. 2 (K. Benirschke, F. M., Garner, and T. C. Jones, Eds.), Springer-Verlag, New York, 1978, pp. 1051–1262.
13. Lemon, P. G., and Gubarova, A. V. Tumours of the ovary. In: Pathology of Tumours in Laboratory Animals (V. S. Turosov, Ed.), IARC, Geneva, 1979, pp. 385–410.
14. Murphy, E. D. Hyperplastic and early neoplastic changes in the ovaries of mice after genic deletion of germ cells. JNCI 48: 1283–1295 (1972).
15. Rehm, S., Dierksen, D., and Deerberg, F. Spontaneous ovarian tumours in Han: NMRI mice: histologic classification, incidence and influence of food restriction. JNCI 72: 1383–1395 (1984).
16. Marchant, J. Animal models for tumours of the ovary and uterus. In: Animal Tumors of the Female Reproductive Tract. Spontaneous and Experimental (E. Cotchin and J. Marchant, Eds.), Springer-Verlag, New York, 1977, pp. 1–25.
17. Latta, J. S., and Pedersen, E. S. The origin of ova and follicle cells from the germinal epithelium of the ovary of the albino rat as demonstrated by selective intravital staining with indian ink. Anat. Rec. 90: 23–35 (1944).
18. Kato, T., Yakushiji, M., Tsunawaki, A., Ide, K., Hirose, N., Araki, S., and Abe, M. Studies on experimental formation of ovarian tumors. Kurume Med. J. 22 (3): 169–176 (1975).
19. Sekiya, S., Endoh, N., Kukuchi, Y., Katoh, T., Matsuura, A., Iawasawa, H., Takeda, B., and Takamizawa, H. *In vivo* and *in vitro* studies of experimental ovarian adenocarcinoma in rats. Cancer Res. 39: 1108–1112 (1979).
20. Cummins, P. A., Fox, H., and Langley, F. A. An electron-microscopic study of the endometrioid adenocarcinoma of the ovary and a comparison of its fine structure with that of normal endometrium and of adenocarcinoma of the endometrium. J. Pathol. 113: 165–173 (1974).
21. Ratcliffe, H. L. Spontaneous tumors in two colonies of rats of the Wistar Institute of anatomy and biology. Am. J. Pathol. 16: 237–254 (1940).
22. Young, R. H., and Scully, R. E. Ovarian Sertoli cell tumors: a report of 10 cases. Int. J. Gynecol. Pathol. 3: 349–363 (1984).
23. Cotchin, E. Spontaneous tumours of the uterus and ovaries in animals. In: Animal Tumours of the Female Reproductive Tract. Spontaneous and Experimental (E. Cotchin and J. Marchant, Eds.), Springer-Verlag, New York, 1977, pp. 26–65.
24. Fredrickson, T. cited by Lingeman, 1974.
25. Nielsen, S., Misdorp, W., and McEntee, K. Tumours of the ovary. Bull. WHO 53: 203–215 (1976).
26. Parmley, T. H., and Woodruff, J. D. The ovarian mesothelioma. Am. J. Obstet. Gynecol. 120 (2): 234–241 (1974).
27. Dallenbach-Hellweg, G. On the histogenesis and morphology of ovarian carcinomas. J. Cancer Res. Clin. Oncol. 107: 71–80 (1984).
28. von Numers, C. Observations on metaplastic changes in the germinal epithelium of the ovary and on the aetiology of ovarian endometriosis. Acta Obstet. Gynecol. Scand. 44: 107–116 (1965).
29. Russell, P. The pathological assessment of ovarian neoplasms. III. The malignant 'epithelial' tumors. Pathology 2: 493–532 (1979).
30. Arias, M., and Aschheim, P. Hypophysectomy and aging primary or secondary ovarian senescence. Experientia 30: 213 (1974).
31. Burek, J. D. Pathology of Aging Rats. CRC Press, Boca Raton, FL, 1978, pp. 117–122.
32. Engle, E. T. Tubular adenomas and testis-like tubules in the ovaries of aged rats. Cancer Res. 6: 578–582 (1946).
33. Frith, C. H., Zuna, R. E., and Morgan, K. A morphologic classification and incidence of spontaneous ovarian neoplasms in three strains of mice. JNCI 67: 693–702 (1981).
34. Thung, P. J., Boot, L. M., and Mühlbock, O. Senile changes in the oestrous cycle and in ovarian structure in some inbred strains of mice. Acta Endocrinol. 23: 8–32 (1956).
35. Fukuishi, R., Wang, H-H., Yoshida, A., Hirota, H., and Mori, H. Induction of ovarian tumour in rats with N-butylnitrosourea. Gann 66: 323–325 (1975).
36. Knowles, J. F. Cancer of rat ovaries: Sertoli cell or granulosa-thecal cell tumours? Br. J. Cancer 48: 301–305 (1983).
37. Arias, M., Scheib, D., and Aschheim, P. Light and electron microscopy of the ovarian interstitial tissue in the senile rat: normal aspect and response to HCG of "deficiency cells" and "epithelial cords." Gerontology 22: 185–204 (1976).
38. Attia, M. A. Neoplastic and nonneoplastic lesions in aging female rats with special reference to the functional morphology of the hyperplastic and neoplastic changes in the pituitary gland. Arch. Toxicol. 57: 77–83 (1985).
39. Meites, J., Huang, H. H., and Simpkins, J. W. Recent studies on neuroendocrine control of reproductive senescence in rats. In: The Aging Reproductive System (E. L. Schneider, Ed.), Raven Press, New York, 1978, pp. 213–236.
40. Reigle, G. D., and Miller, A. E. Aging effects on the hypothalamic-hypophyseal-gonadal control systems. In: The Aging Reproductive System (E. L. Schneider, Ed.), Raven Press, New York, 1978, pp. 159–192.
41. Ashley, D. J. B. Evans' Histological appearances of tumours. Churchill Livingstone, Edinburgh, 1978, pp. 663–672.
42. Norris, H. J., Garner, F. M., and Taylor, H. B. Comparative pathology of ovarian neoplasms. IV. Gonadal stromal tumours of canine species. J. Comp. Pathol. 80: 399–405 (1970).
43. Deane, H. W., Lobel, B. L., and Romney, S. L. Enzymic histochemistry of normal human ovaries of the menstrual cycle, pregnancy, and the early puerperium. Am. J. Obstet. Gynecol. 83: 281–295 (1962).
44. Demopoulos, R. I., and Kammerman, S. Fine structural evidence on the origin of gonadotropin induced ovarian tumors in mice. Cancer Res. 41: 871–876 (1981).
45. Hamlett, J. D., Aparicio, S. R., and Lumsden, C. E. Light and electron microscope studies on experimentally induced tumours of the theca-granulosa cell series in the mouse. J. Pathol. 105: 111–124 (1971).
46. Dehner, L. P., Norris, H. J., Garner, F. M., and Taylor, H. B. Comparative pathology of ovarian neoplasms. III. Germ cell tumours of canine, bovine, feline, rodent and human species. J. Comp. Pathol. 80: 299–310 (1970).
47. Haseman, J. K., Huff, J., and Boorman, G. A. Use of historical control data in carcinogenicity studies in rodents. Toxicol. Path. 12: 126–132 (1984).

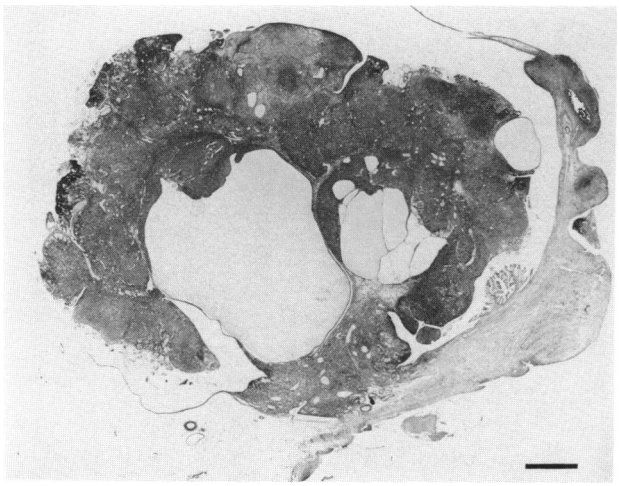

PLATE 1. Low power photomicrograph of tubular adenoma. Note short papillomatous projections along surface of tumor. H&E. Bar = 1 mm.

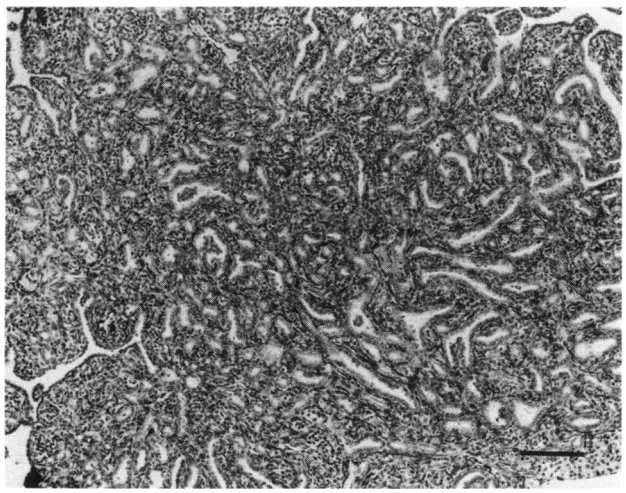

PLATE 2. Tubular adenoma. Tumor composed of narrow tubules lined by cuboidal cells. H&E. Bar = 100 μm.

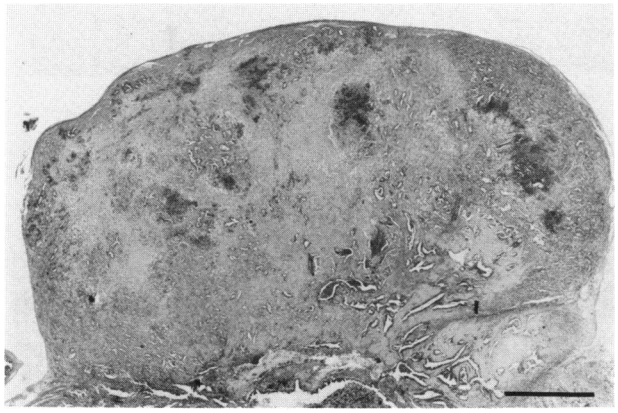

PLATE 3. Anaplastic adenocarcinoma. Irregular tubules and abundant stroma. H&E. Bar = 1 mm.

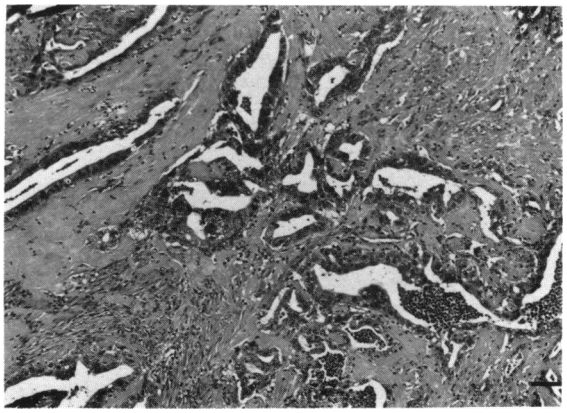

PLATE 4. Anaplastic adenocarcinoma. Irregular tubules of anaplastic cells with inflammatory cell infiltration and abundant stroma. H&E. Bar = 100 μm.

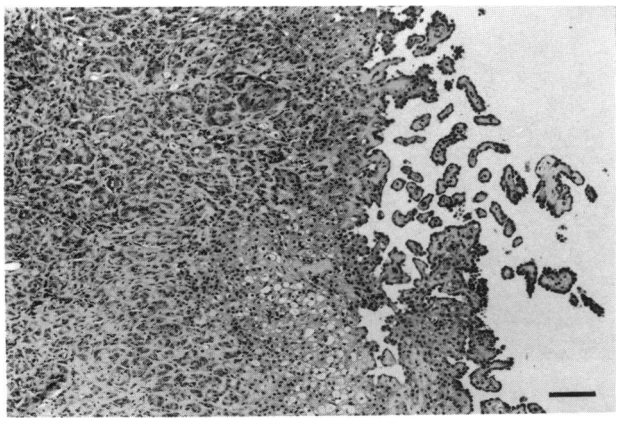

PLATE 5. Mesothelioma. Primary tumor illustrating tubulopapillary pattern. H&E. Bar = 100 μm.

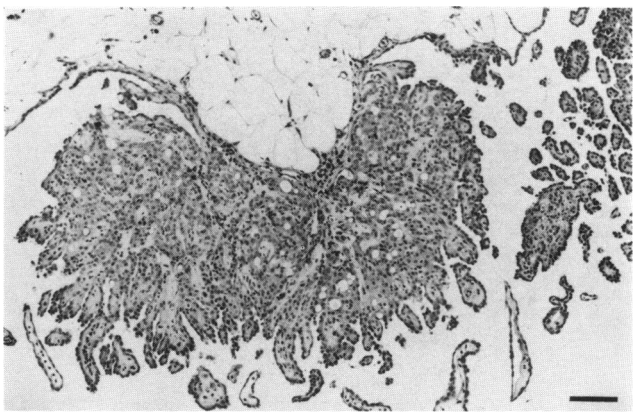

PLATE 6. Mesothelioma. Secondary deposits from abdominal adipose tissue. H&E. Bar = 100 μm.

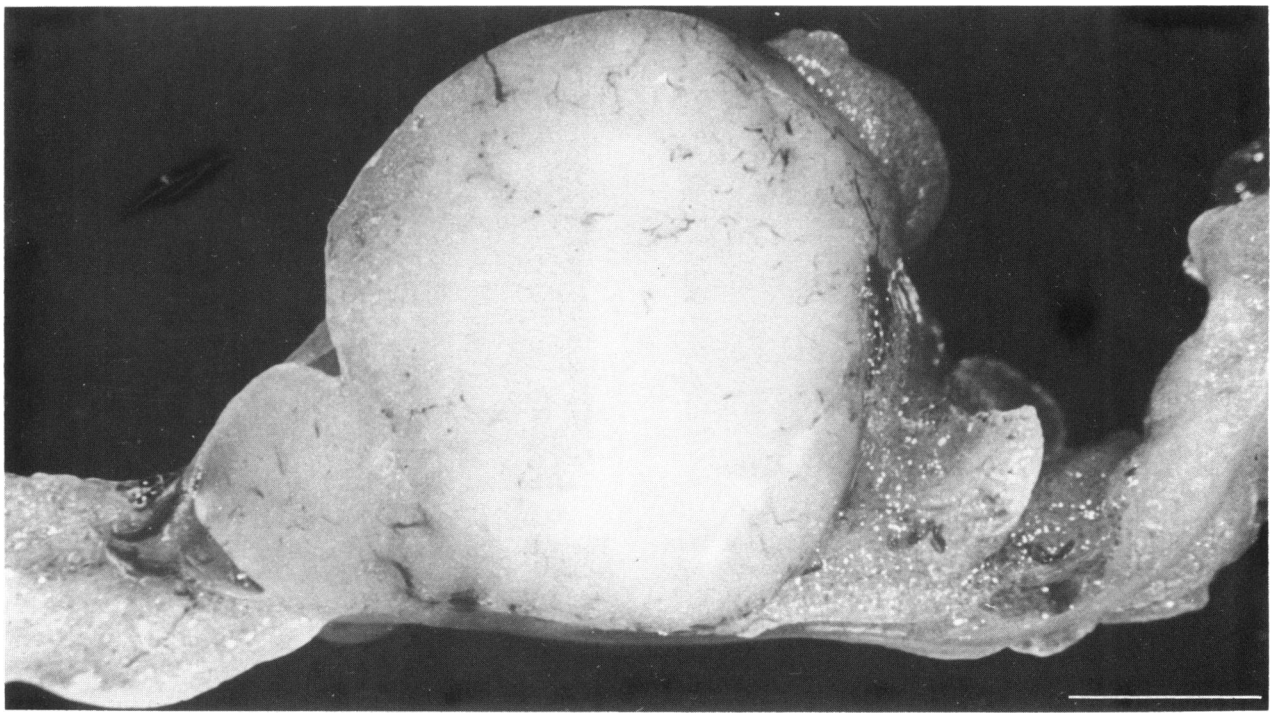

PLATE 7. Sertoliform tubular adenoma. Macrophotograph. Pale mass occupying whole ovary. Bar = 2 mm.

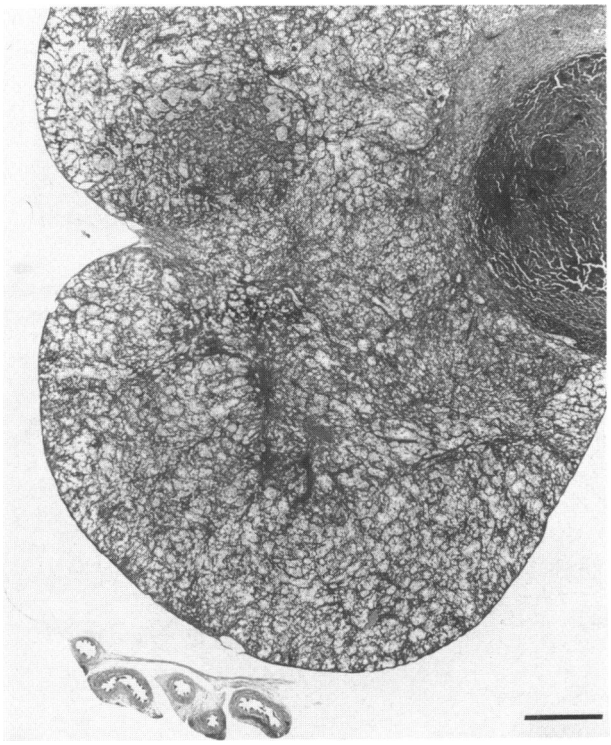

PLATE 8. Sertoliform tubular adenoma. Low power photomicrograph showing complete replacement of ovarian structure by pale tubules. H&E. Bar = 1 mm.

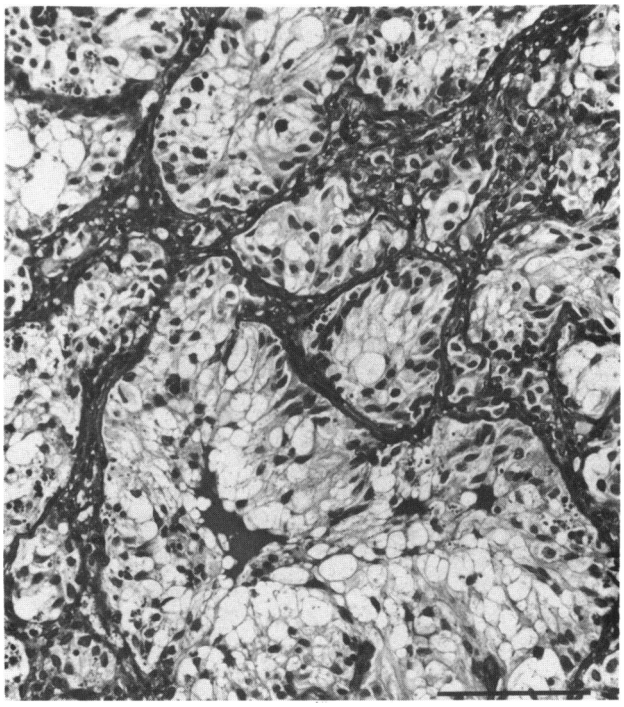

PLATE 9. Sertoliform tubular adenoma. Irregular tubules composed of pale vacuolated cells with round inclusions. PAS, hematoxylin. Bar = 100 μm.

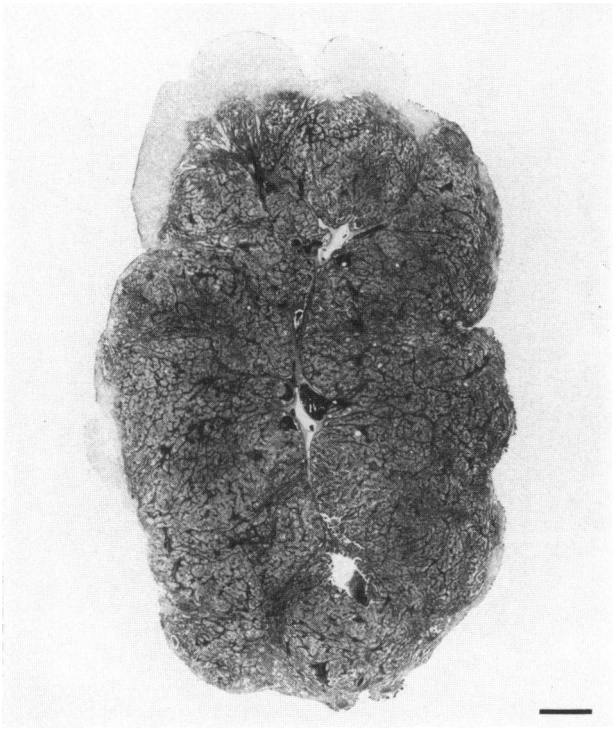

PLATE 10. Sertoli's cell tumor. Low power photomicrograph to show pronounced tubular pattern. H&E. Bar = 1 mm.

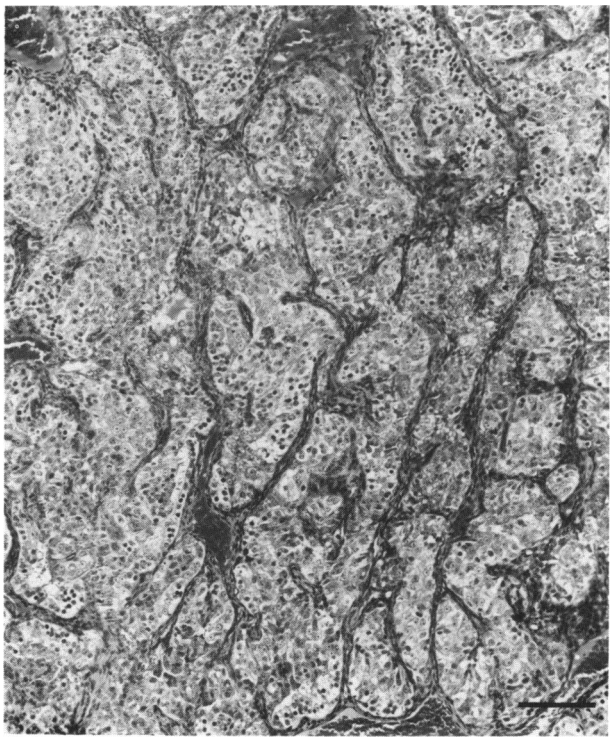

PLATE 11. Sertoli's cell tumor. Solid tubules with fine peritubular stroma. H&E. Bar = 100 μm.

PLATE 12. Sertoli's cell tumor. Junction between tubular structures and area with palisaded appearance. H&E. Bar = 200 μm.

PLATE 13. Sertoli's cell tumor. Areas of palisaded cells and sertoliformlike tubules. H&E. Bar = 200 μm.

PLATE 14. Granulosa cell tumor. Macrophotograph. Large pale mass. Bar = 10 mm.

PLATE 15. Malignant granulosa cell tumor. Areas of hemorrhage, cysts, and prominent pale areas of lutein cells. H&E. Bar = 1 mm.

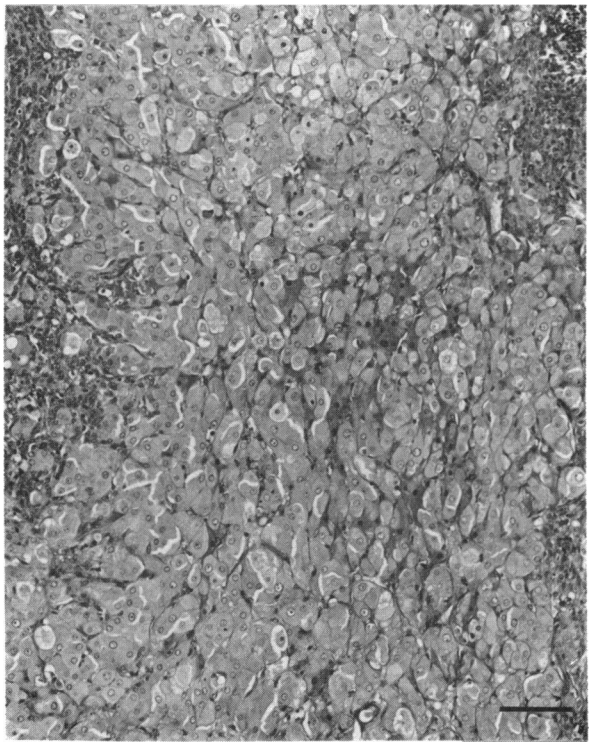

PLATE 16. Malignant granulosa cell tumor. Large, pale lutein cells. H&E. Bar = 100 μm.

PLATE 17. Malignant granulosa cell tumor. Large metastatic pulmonary deposit. H&E. Bar = 1 mm.

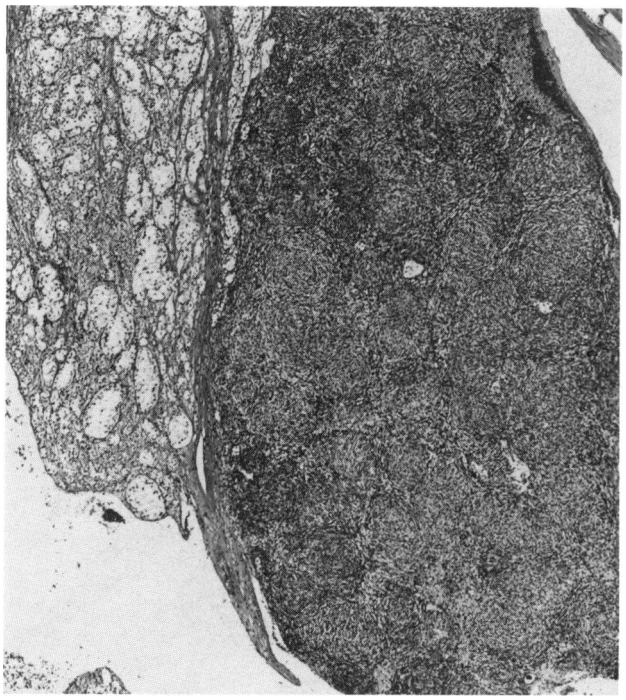

PLATE 18. Thecal cell tumor. Small, well-differentiated tumor with nodular appearance. Adjacent sertoliform tubules. H&E. Bar = 200 μm.

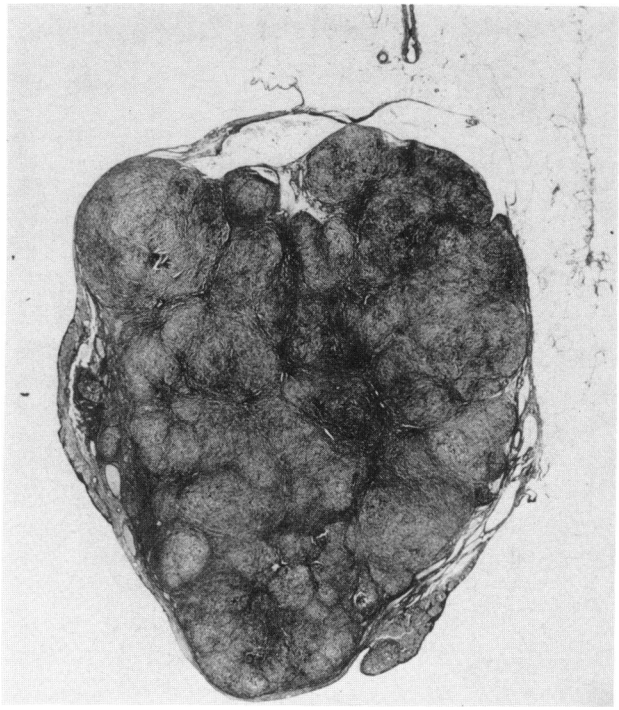

PLATE 19. Thecal cell tumor. Low power photomicrograph to show pronounced whorled, nodular appearance. Reticulin stain. Bar = 1 mm.

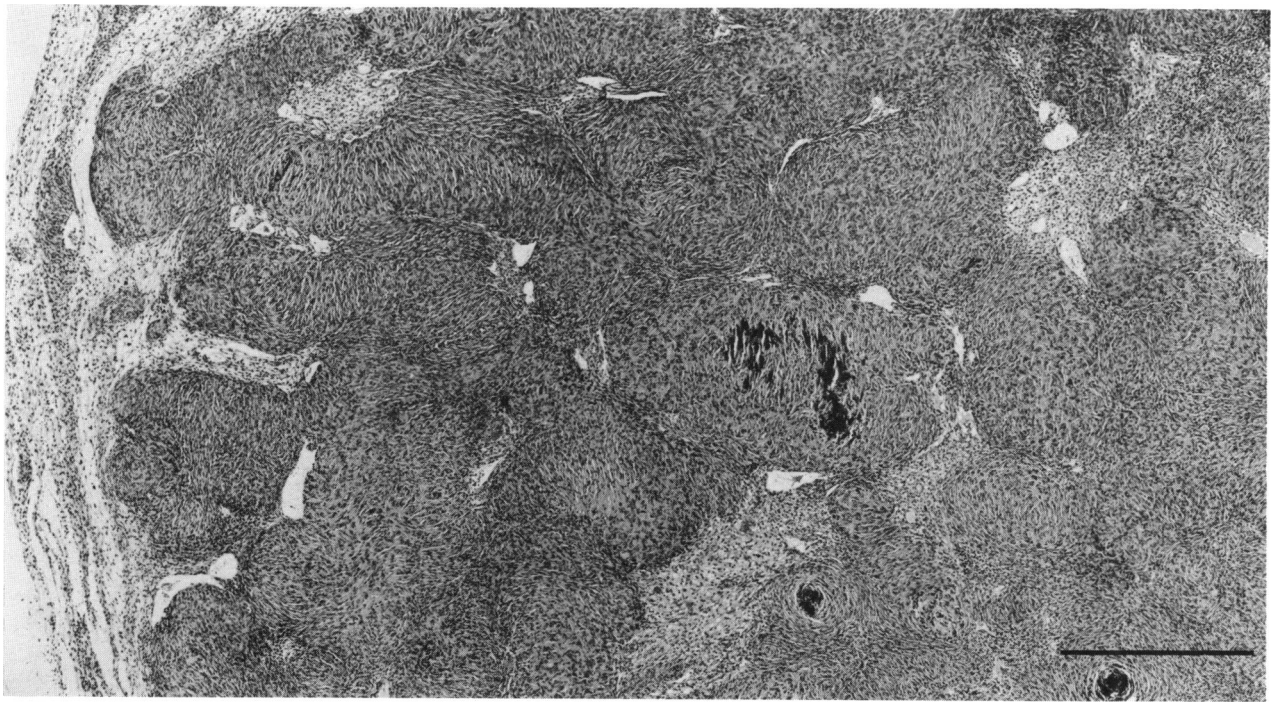

PLATE 20. Thecal cell tumor. Nodular pattern with focal mineralization. H&E. Bar = 1 mm.

PLATE 21. Polycystic sex cord-stromal tumor. Macrophotograph. Tumor composed numerous pale, thin-walled cysts. Bar = 25 mm.

PLATE 22. Polycystic sex cord-stromal tumor. Variable sized cysts and pale interstitial cells. H&E. Bar = 200 μm.

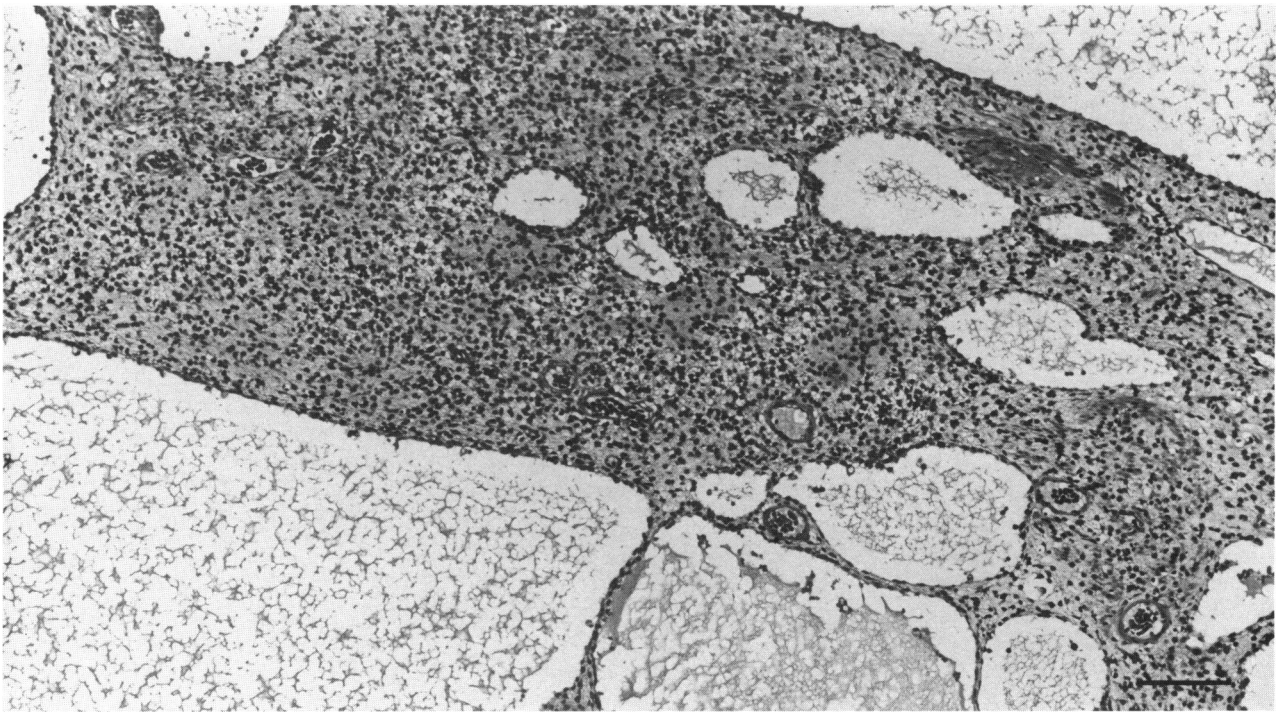

PLATE 23. Polycystic sex cord-stromal tumor. Cysts lined by thin cells. Interstitial cells have slightly vacuolated appearance in this field. H&E. Bar = 100 μm.